



Molecular Crystals and Liquid Crystals

Publication details, including instructions for authors and subscription information:

<http://www.tandfonline.com/loi/gmcl20>

CUBIC AND BLUE PHASES IN A FLUORINE-CONTAINING DICHIRAL COMPOUND

Yoichi Takanishi^a, Shohei Yoshida^a, Toyokazu Ogasawara^a, Ken Ishikawa^a, Hideo Takezoe^a, Kenji Ema^b, Haruhiko Yao^b, Atsushi Yoshizawa^c, Tetsuo Kusumoto^d & Tamejiro Hiyama^e

^a Department of Organic and Polymeric Materials, Tokyo Institute of Technology, O-okayama, Meguro-ku, Tokyo 152-8552, Japan

^b Department of Physics, Tokyo Institute of Technology, O-okayama, Meguro-ku, Tokyo 152-8552, Japan

^c Department of Materials Science and Technology, Hirosaki University, Hirosaki 036-8561, Japan

^d Dainippon Ink & Chemicals, INC., Komuro, Ina-machi, Kitaadachi-gun, Saitama 362-8557, Japan

^e Department of Material Chemistry, Graduate School of Engineering, Kyoto University, Yoshida, Kyoto 606-8501, Japan

Version of record first published: 15 Jul 2010

To cite this article: Yoichi Takanishi, Shohei Yoshida, Toyokazu Ogasawara, Ken Ishikawa, Hideo Takezoe, Kenji Ema, Haruhiko Yao, Atsushi Yoshizawa, Tetsuo Kusumoto & Tamejiro Hiyama (2003): CUBIC AND BLUE PHASES IN A FLUORINE-CONTAINING DICHIRAL COMPOUND, *Molecular Crystals and Liquid Crystals*, 401:1, 19-33

To link to this article: <http://dx.doi.org/10.1080/744814913>

PLEASE SCROLL DOWN FOR ARTICLE

Full terms and conditions of use: <http://www.tandfonline.com/page/terms-and-conditions>

This article may be used for research, teaching, and private study purposes. Any substantial or systematic reproduction, redistribution, reselling, loan, sub-licensing, systematic supply, or distribution in any form to anyone is expressly forbidden.

The publisher does not give any warranty express or implied or make any representation that the contents will be complete or accurate or up to date. The accuracy of any instructions, formulae, and drug doses should be independently verified with primary sources. The publisher shall not be liable for any loss, actions, claims, proceedings, demand, or costs or damages whatsoever or howsoever caused arising directly or indirectly in connection with or arising out of the use of this material.

CUBIC AND BLUE PHASES IN A FLUORINE-CONTAINING DICHIRAL COMPOUND

*Yoichi Takanishi, Shohei Yoshida, Toyokazu Ogasawara,
Ken Ishikawa and Hideo Takezoe*
*Department of Organic and Polymeric Materials,
Tokyo Institute of Technology, O-okayama, Meguro-ku,
Tokyo 152-8552, Japan*

Kenji Ema and Haruhiko Yao
*Department of Physics, Tokyo Institute of Technology,
O-okayama, Meguro-ku, Tokyo 152-8552, Japan*

Atsushi Yoshizawa
*Department of Materials Science and Technology,
Hirosaki University, Hirosaki 036-8561, Japan*

Tetsuo Kusumoto
*Dainippon Ink & Chemicals, INC., Komuro, Ina-machi,
Kitaadachi-gun, Saitama 362-8557, Japan*

Tamejiro Hiyama
*Department of Material Chemistry, Graduate School
of Engineering, Kyoto University, Yoshida,
Kyoto 606-8501, Japan*

The structure and dynamics in an optically isotropic liquid crystalline phase exhibited in a dichiral compound with fluorines have been investigated using X-ray, ¹⁹F-NMR and dielectric measurements. Results in the dielectric measurement and ¹⁹F-NMR measurements clearly show that molecular motion in this phase is just like in the isotropic phase as observed by texture. However, several X-ray diffraction peaks observed in a small angle range indicate

We acknowledge stimulating discussion with Prof. P. Toledano during his stay in TIT. This work is partly supported by ASET and a Grant-in-Aid for Scientific Research on Priority Area (B) (12129202) and for an Encouragement of Young Scientists (11750008), by the Ministry of Education, Science, Sports and Culture. This work was carried out under the approval of the Photon Factory Advisory Committee (Proposal No. 98G341 and No. 00G088).

a kind of cubic phase (Cub). Based on the X-ray diffraction patterns together with the existence of circular dichroism, the phase is assigned to a chiral cubic structure belonging to crystallographic spacegroup $I432$. Moreover, the exotic phase with blue colored and foggy texture was found in the lower temperature range of isotropic liquid. X-ray diffraction in this phase clearly shows a diffraction ring corresponding to a layer structure, indicating that this blue-colored phase is assignable to a smectic blue phase (BP_{sm}). It was also found that the layer correlation length is remarkably long compared with the previously reported BP_{sm} phases. We want to emphasize that the present material is quite unique in the sense that both cubic phases, BP_{sm} and Cub, appear. The influence of cell thickness and incubation time on the emergence of the smectic C^ phase is also discussed based on dielectric measurements and AC calorimetry.*

Keywords: cubic phase; blue phase; dynamics; X-ray; ac calorimetry

1. INTRODUCTION

Liquid crystalline compounds are interesting soft materials from both viewpoints of fundamental science and application to electrooptic switching devices. In particular, the study of chirality in the liquid crystalline phases becomes much more attractive. Chirality sometimes induces complex phase structures. One of them is the twist grain boundary (TGB) phase, where smectic blocks form a helix with the helical axis parallel to the smectic layer and with an array of screw dislocations inbetween[1]. The other unique molecular arrangement organized by chirality is the blue phase (BP)[2], that emerges, since molecules have a chance to form a helix to any directions perpendicular to the molecular rod, when cholesteric helix emerges three-dimensionally in the isotropic phase. BP appearing between the isotropic (Iso) and chiral nematic (N^*) phases is well-known. In addition, the smectic analogue of BP was discovered recently [3,4] and was designated as BP_{sm} [5]. However, only a few materials showing the BP_{sm} phase are known.

In addition to these BP and BP_{sm} phases with cubic structures, another type of cubic phase (Cub) appears in the liquid crystalline system possessing strong tendency to aggregate via many types of intermolecular interactions[6]. Although extensive studies have been made on the Cub phase, only a very few chiral materials that show the Cub phase are known in thermotropic liquid crystals. Particularly there is only one material that exhibits both cubic phases, i.e., BP and Cub. In the material, Cub appears only monotropically[7]. Hence we can say that there is no material that stably exhibits both cubic phases.

This paper describes a novel dichiral material that has both cubic phases. First, we represent the dynamic aspect of molecules in the Cub

phase based on ^{19}F -NMR spectroscopy and dielectric measurements. The X-ray analysis together with the existence of circular dichroism tells us that Cub is assignable to I432 and BP is actually BP_{sm} with a fairly long correlation length of layer order.

2. EXPERIMENTAL

The sample used was a fluorine-substituted dichiral molecule, 2-[4-((*R*)-2-fluorohexyloxy)phenyl]-5-[4-((*S*)-2-fluoro-2-methyldecanoyloxy)phenyl]pyrimidine ((*R*, *S*)-FPPY)[8–11], whose chemical structure and phase sequence are shown in Figure 1. For dielectric measurements, $2 \sim 14\mu\text{m}$ thick planar cells prepared by rubbing method after coating polyimide were used. The measurements were performed using an impedance analyzer HP4192A (HP) with an oscillation amplitude of ca $1\text{mV}/\mu\text{m}$ and a frequency range of $5\text{Hz} \sim 13\text{MHz}$. We controlled the temperature of the samples using a heater block and a temperature controller (Chino, DB1230) within an accuracy of $\pm 0.1^\circ\text{C}$. Texture observation of these cells was made using a polarizing optical microscope (NIKON OPTIPHOT-POL).

^{19}F -NMR measurements were carried out using a high resolution solid state nuclear magnetic resonance spectrometer, CMX-300WB (Chemag-netics). The resonance frequency for fluorine 19 is 287 MHz (7T). The sample was put in a 4mm^ϕ zirconia tube. In the T_1 and MAS measurements, it was rotated at 8 kHz using the magic-angle-spinning (MAS) method with proton decoupling. In the measurement of the spin-lattice relaxation time T_1 , we used the inversion recovery technique [12], the pulse sequence of which was $180^\circ - \tau - 90^\circ - \text{acq}(+)$ and after a pulse delay time (*pd*) $90^\circ - \text{acq}$ and *pd*. In the measurements, we set the 90° pulse width to $2\mu\text{s}$, *pd* between each acquisition to 6.0 s, accumulation time to 3160, and τ to 0.1, 0.2, 0.4 and 0.7 s. The static measurement without sample spinning was

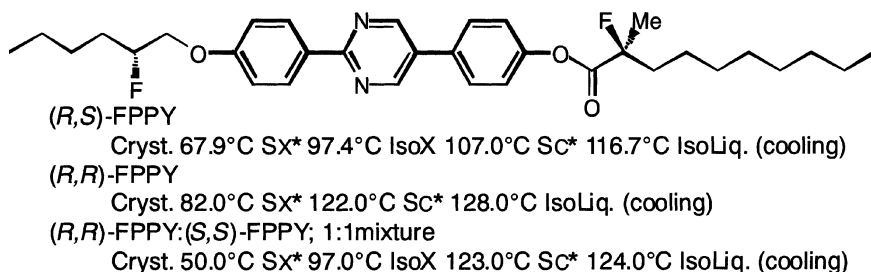


FIGURE 1 Chemical structure of dichiral compound with fluorines, FPPY, and the phase sequences of its (*R*, *S*)-, (*R*, *R*)-, (*S*, *S*)-forms and their mixture.

also carried out[13]. In this measurement, normal 90° pulse with proton decoupling technique was used, and 90° pulse width was $1.5\mu\text{s}$. The temperature of the sample tube was controlled using temperature-regulated air, and its accuracy was better than $\pm 1^\circ\text{C}$ and $\pm 0.5^\circ\text{C}$ in the MAS and T_1 measurements and the static measurement, respectively. Cooling and heating rates in these measurements were about $1^\circ\text{C}/\text{min}$. We waited for about 10 min before starting the measurements at each temperature.

X-ray diffraction measurements were conducted using two setups; i.e., a commercial X-ray system (Rigaku, RU-200) and a synchrotron radiation system of Photon Factory in Tsukuba. Samples were introduced into various types of cells, such as $100\sim 350\mu\text{m}$ thick sandwich cells and $25\mu\text{m}$ thick free surface films for the former system, while 1mm^ϕ capillary tube samples were used for the latter system. Only preliminary data were acquired by the former system, since diffraction profiles changed by sample preparation and repeated measurements. Hence we used the latter system for the quantitative determination of the diffraction angles in Cub, since the data acquisition is made in a short time because of strong light source. The X-ray energy was monochromated to 8keV ($\lambda = 1.55\text{\AA}$) and the incident beam was collimated using a Si/W multilayer monochromator and focusing mirror with an angular divergence of 0.5mrad , and the spatial resolution was $3\times 3\mu\text{m}^2$. The optical geometry used is the same as that previously reported [14,15] except using an imaging plate (IP) instead of a one-dimensional scintillation counter, so that we can rapidly obtain a two-dimensional diffraction pattern. The exposure time was $5\sim 30\text{s}$. Camera length was calibrated using the lattice constants of stearic acid measured in the same condition.

The heat capacity was measured using an AC calorimeter described previously[16]. The sample of 22.2mg was hermetically sealed in gold cells. The temperature was scanned with a rate of about $2.5\text{mK}/\text{min}$.

3. RESULTS AND DISCUSSION

3.1 Dynamics in Cubic Phase

3.1.1 Dielectric Measurements

In order to investigate electric properties and molecular dynamics, dielectric measurements were carried out. The preliminary results have been reported in our previous paper[10]. Figure 2 shows the temperature dependences of the dielectric constant (real part) at 5kHz in the planar cells with various cell gaps. In a $4.4\mu\text{m}$ thick cell, relatively large values of real component of dielectric constants were observed in the SmC^* and SmX^* phases, while those in the IsoX phase were very small like in iso-

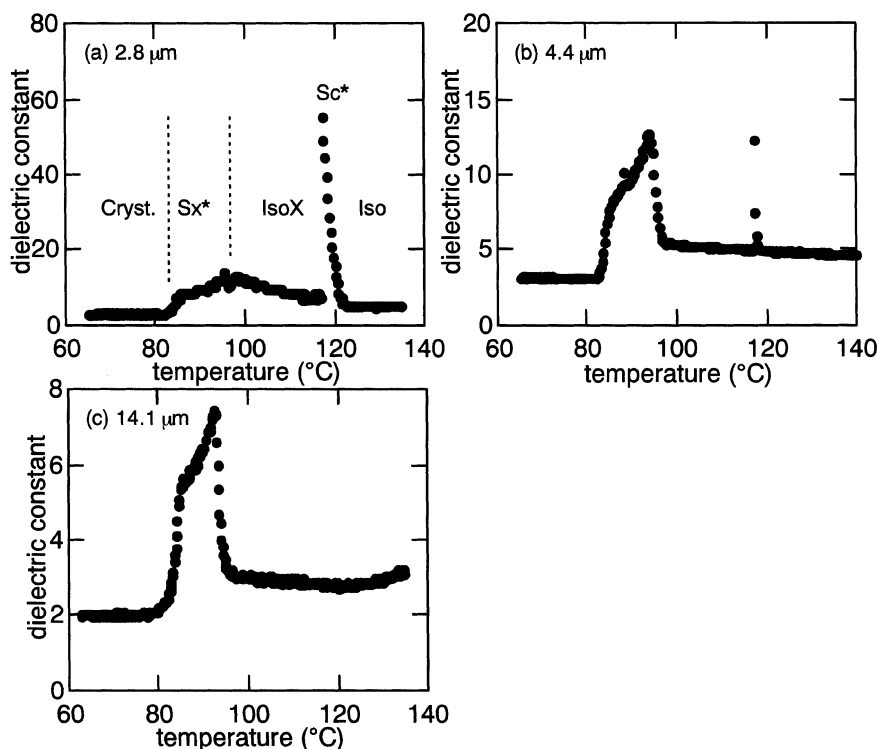


FIGURE 2 Temperature dependence of the dielectric constant (real component) of (*R, S*)-FPPY at 5 kHz. Cell thicknesses used were (a) 2.8, (b) 4.4 and (c) 14.1 μm .

tropic liquid (IsoLiq.). Actually, the values in IsoX and IsoLiq. continuously change with temperature except for the anomaly in SmC*. This result indicates that the dielectric property in IsoX is paraelectric.

Phase sequence slightly depends on the cell thickness; The SmC* phase is not observed in thicker cells, as shown in Figure 2(c). Although the dielectric constant in a 2.8 μm thick cell was relatively high in the IsoX phase region (110 ~ 118 °C) compared with that in thicker cells, the IsoX phase was confirmed to exist by texture observation. Small smectic clusters remained at surfaces may be responsible for the finite dielectric constant.

Figure 3 shows the frequency dispersions of dielectric constants in each phase of the 4.4 μm thick cell. The relaxation in the vicinity of 1 MHz observed even in IsoLiq. is due to ITO electrodes. In the SmC* phase, a relaxation mode was observed at ca. 10 kHz, which may correspond to the Goldstone mode. In IsoX, on the other hand, small dielectric constants

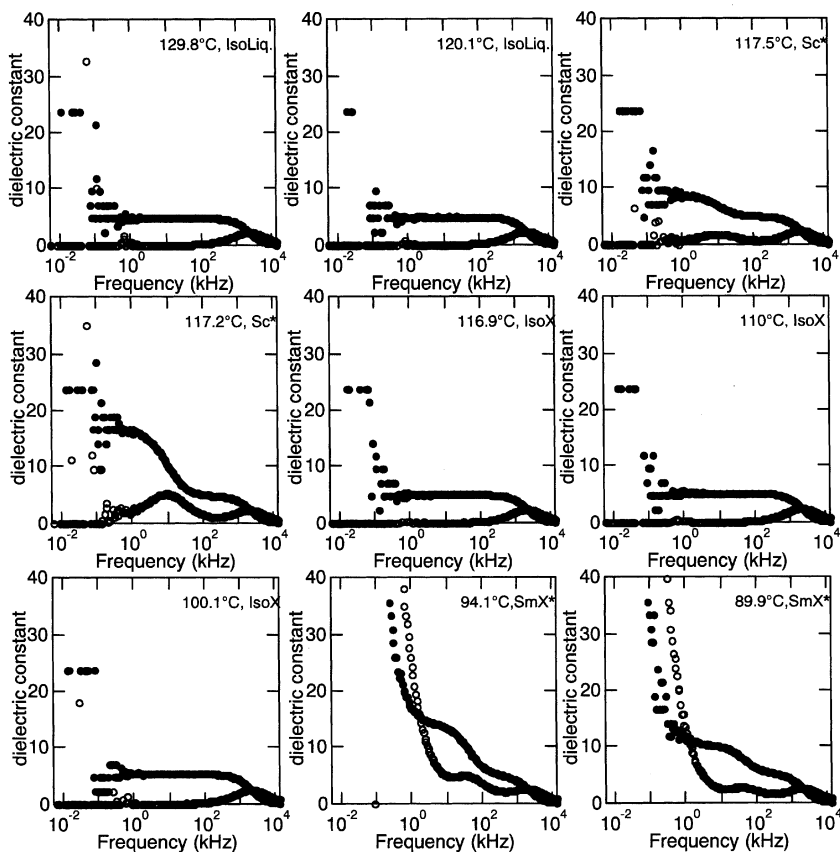


FIGURE 3 Frequency dispersion of the dielectric permittivity in each phase of a 4.4 μm thick cell. Note that the profiles in IsoLiq. and IsoX are very similar.

without any relaxation were observed, as observed in IsoLiq. In the SmX* phase, two relaxation modes appear at less than 100 Hz and 30 kHz. The higher frequency mode may correspond to the Goldstone mode, the same as observed in SmC*. Although the lower frequency mode cannot be assigned, this result suggests that the SmX* phase would be different from the SmC* phase.

3.1.2 ^{19}F -NMR Measurements

Figure 4(a) shows the temperature dependence of the isotropic chemical shifts of two fluorines in the magic angle spinning (MAS) measurement. As a reference, the isotropic chemical shift of fluorine of CFCl_3 was defined as 0 ppm. In the whole temperature range of the experiment, their

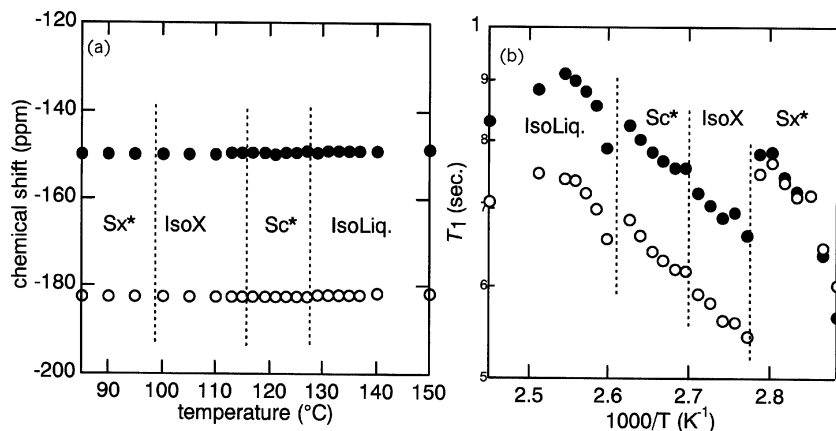


FIGURE 4 (a) Temperature dependence of the isotropic chemical shifts of two fluorines of (*R*, *S*)-FPPY in the magic angle spinning (MAS) measurement. The value of chemical shift was determined using F-rubber as a reference, -69 ppm. (b) Temperature dependence of T_1 relaxation time of two fluorine nuclei of (*R*, *S*)-FPPY. Open and closed circles correspond to those in (a), respectively.

chemical shifts hardly changed, suggesting that the molecular conformation around the chiral parts and their chemical circumstance does not change at the phase transitions.

Figure 4(b) shows the temperature dependence of the spin-lattice relaxation time T_1 of two fluorine nuclei. Although certain discontinuous jumps were observed at each phase transition, the value of T_1 in the IsoX phase monotonically decreases with decreasing temperature. T_1 in the phase boundary of IsoX is slightly larger than that in the neighboring phases, i.e., the lower temperature side of SmC* and the higher temperature side of SmX*. This fact suggests that the molecular motion in IsoX is more rapid than that in the neighboring phases, as in IsoLiq.

Figure 5 shows the static ^{19}F -NMR spectra in each phase. Two sharp peaks assigned to two fluorines in the vicinity of chiral carbon were observed in IsoLiq. as shown in Figures 5(a) and 5(e). In the IsoLiq. phase, the value of chemical shifts and the spectral shape are almost the same as those in the MAS measurement. When the IsoLiq.-SmC* phase transition occurs, two small peaks in addition to the large peaks already observed in IsoLiq. appear in the lower field shift side, as shown in Figure 5(b). It suggests that molecules align due to a high magnetic field and that the chemical shift anisotropy exists. This profile is the same as that in SmC* of stereoisomers, (*R*, *S*)-FPPY, (*S*, *S*)-FPPY (see Figure 5(f) and 5(g)). When the phase transition to IsoX occurred, the spectrum almost

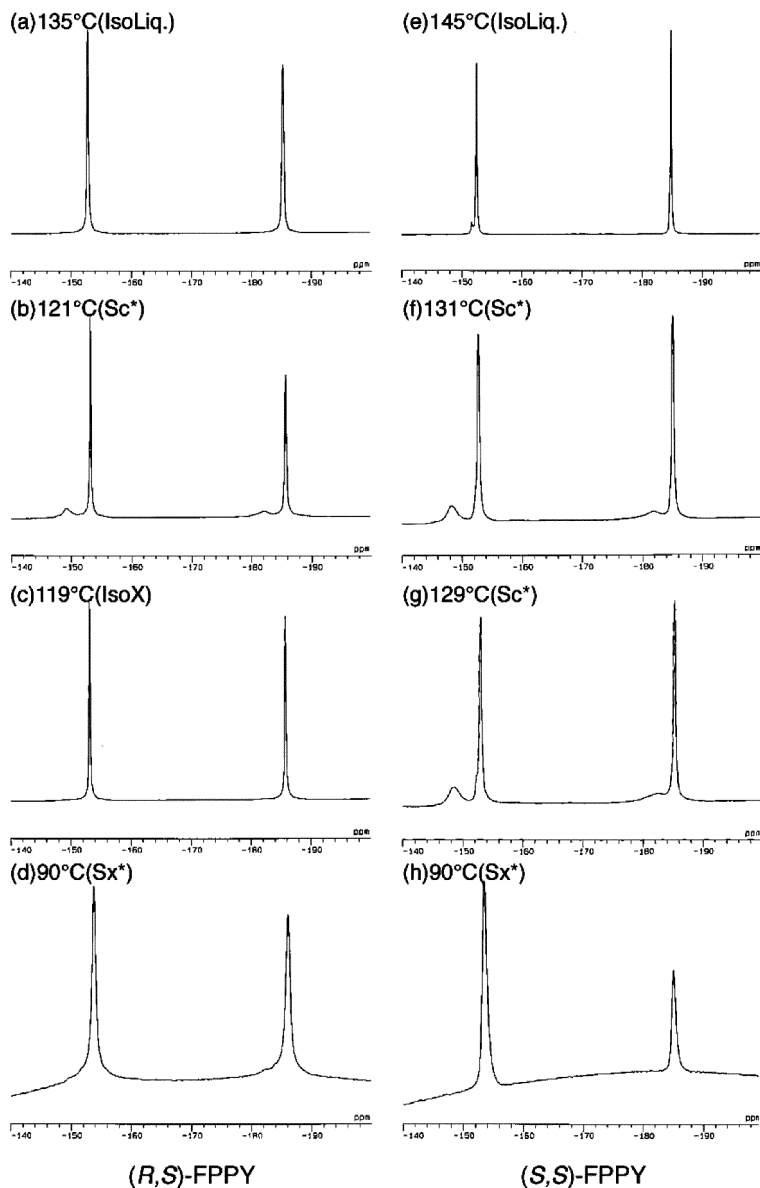


FIGURE 5 ^{19}F -NMR spectra in each phase of (*R,S*)-FPPY ((a) ~ (d)) and (*S,S*)-FPPY ((e) ~ (h)). They were obtained using a static oriented sample.

returned to that in the IsoLiq. phase, although we could expect some profile changes due to inter- and intra-molecular interactions. These results indicate that the molecular motion in the IsoX phase is very rapid and isotropic as in IsoLiq. at the NMR frequency. Considering the results of the dielectric and NMR measurements, the molecular behavior is quite similar to that in IsoLiq., though the viscosity in the IsoX phase is much higher than that in IsoLiq.

3.2 Structure of the Cubic Phase

3.2.1 X-ray Diffraction Measurements using a Commercial System

Let us first show the X-ray profiles obtained using a commercial X-ray diffraction system for homeotropically aligned free surface films with a thickness of 25 μm and 350 μm thick sandwich cells prepared with homeotropic alignment treatment. Figures 6(a) ~ 6(c) and 6(d) ~ 6(f) show the diffraction profiles in the conventional 2θ - θ method, and the rocking curves in the ω -scanning measurement at the smallest diffraction angle $2\theta_{\text{B}}$, respectively. In Figure 6(b), two peaks were observed at $2\theta_{\text{B}} = 3.23^\circ$ and 3.72° in IsoX and the smaller $2\theta_{\text{B}}$ is close to that corresponding to the layer thickness in SmC* (Figure 6(a)). Rocking curve of ω -scanning indicates a sharp single peak, suggesting that the lattice corresponding to the diffraction peak at $2\theta_{\text{B}} = 3.23^\circ$ is almost homeotropically oriented. Thus, this lattice seems to be a kind of the smectic layer. Actually, we first speculated so, as mentioned in our previous paper[8]. However, this is not actually the case, as will be mentioned in the following. We made similar measurements using a 350 μm thick sandwich cell in which substrate surface was treated for homeotropic alignment. The results are shown in Figure 7. In addition to the two peaks already observed in the measurement using a free surface film, the other two peaks were observed at $2\theta = 2.93^\circ$ and 3.48° , as shown in Figure 7(a) or 7(b). Figures 7(d) and 7(e) are rocking curves of ω -scanning measurement in which the detector was fixed at $2\theta = 3.224^\circ$ and 3.724° , respectively. Figures 7(a) and 7(b) were actually taken after changing the condition between 2θ and $\theta(\omega)$. In the transmission geometry measurement, in which the direction of the incident X-ray beam is almost normal to the substrates, other peaks appear, as shown in Figure 7(c). These results suggest that the IsoX phase does not have a simple smectic layer structure but has a three-dimensional lattice. Considering optically isotropic property and 3D lattice, IsoX would form a cubic structure[17].

For quantitative analysis we tried to collect the diffraction angles in the IsoX phase. However, it was very difficult to determine its structure using a commercial X-ray system because of the temporal change of the

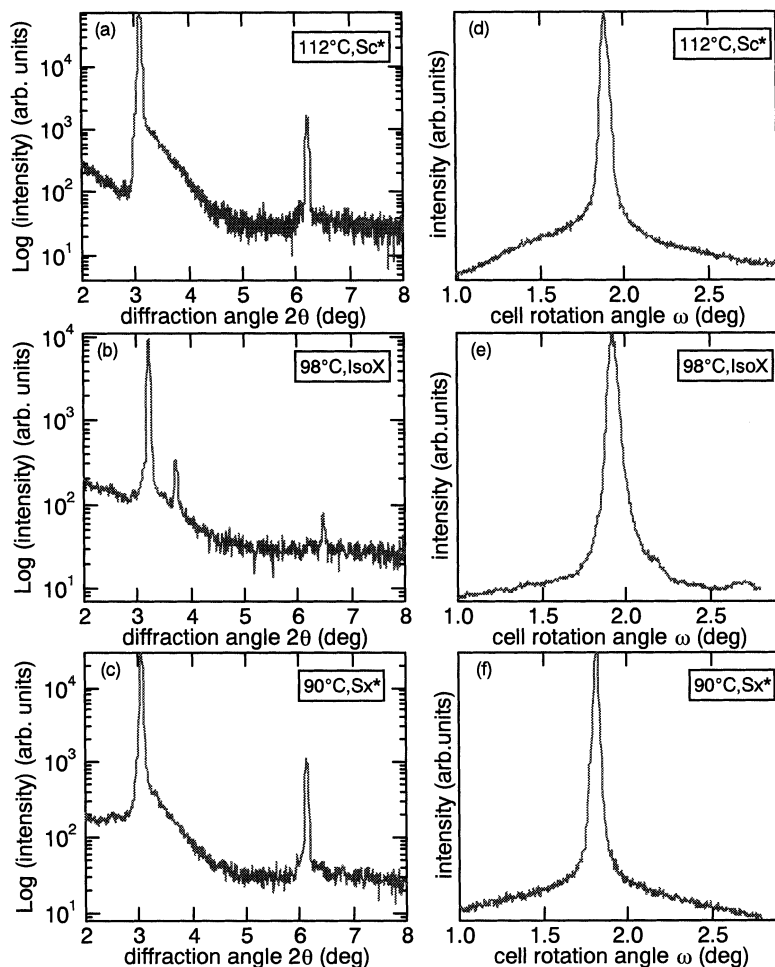


FIGURE 6 Diffraction profiles in a 25 μ m thick free surface film of (*R*, *S*)-FPPY in the conventional 2θ - θ method ((a)–(c)) and the corresponding rocking curves of ω -scanning ((d)–(f)).

diffractions. Hence we decided to use synchrotron X-ray source, as suggested by Levelut and Clerc [18].

3.2.2 X-ray Diffraction Measurements using a Synchrotron X-ray Microbeam

As mentioned above, quick data acquisition from uniform domains is important. One of the solutions for this problem is the use of a synchrotron radiation. For this reason, we measured the X-ray microbeam diffraction

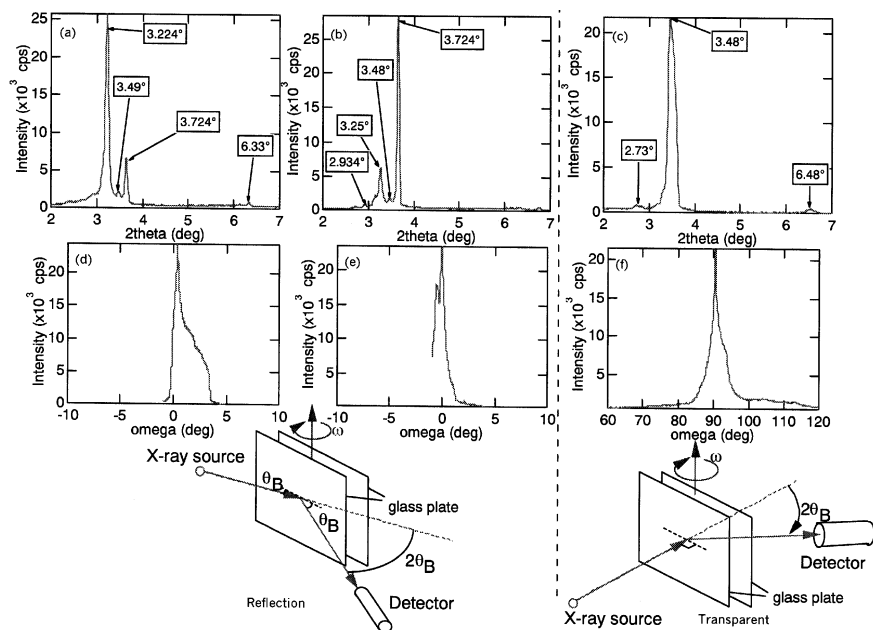


FIGURE 7 2θ - θ diffraction profiles of a 350 μ m thick glass sandwich cell of (*R, S*)-FPPY at 110°C as satisfying the relation between 2θ and ω as follows; (a) $2\theta = 3.224^\circ$ and $\omega = 0.38^\circ$, (b) $2\theta = 3.724^\circ$ and $\omega = -0.05^\circ$. ω -scanning rocking curves observed at $2\theta = 3.224^\circ$ (d) and 3.724° (e). Diffraction profiles in the 2θ - θ method as obtained in transmission geometry (c) and the rocking curves at $2\theta = 3.48^\circ$ (f).

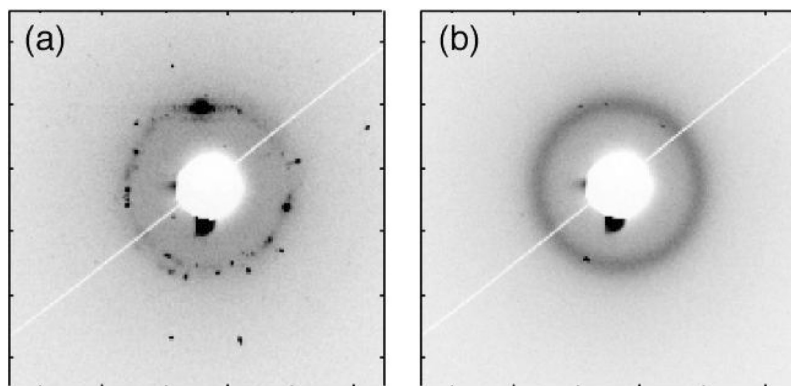


FIGURE 8 2-dimensional x-ray diffraction pattern of (*R, S*)-FPPY using an X-ray microbeam. (a) 125°C (IsoX) and (b) 130°C (BP_{sm}).

from the uniformly oriented samples. Obtained two-dimensional X-ray diffraction patterns are shown in Figure 8.

The pattern shown in Figure 8(a) was taken in the IsoX phase (125.5°C) on gradual cooling from IsoLiq. The diffraction patterns are rather simple, which suggests that the diffraction is obtained from domains comparable with or larger than the beam spot size. From the diffraction profile, we calculated the reciprocal distances of IsoX. By comparing the data with the calculated ones assuming the space group of $Im\bar{3}m$ or $I432$ with a unit lattice constant of 93.9Å, we obtained a good agreement[11]. We also found that the cubic phase clearly exhibits circular dichroism[11]. Hence we concluded that the IsoX phase is assigned to a chiral cubic phase with symmetry of $I432$. Assuming a density of 1g/cm^3 , there are ca. 900 molecules per cubic unit cell.

3.3 AC Calorimetry

As mentioned in Figure 2, the SmC^* phase is a very unstable phase; the temperature range of SmC^* seriously depends on cell thickness. It was also found that the phase transition from SmC^* to IsoX occurs with an endothermic peak in DSC measurements, indicating that SmC^* is a metastable state. The abnormal character of the SmC^* phase was also observed in AC calorimetry as complicated and unreproducible variation of heat capacity with temperature[19]. Another experimental observation is that the width of the SmC^* phase depends on the history of the sample temperature variation. When the sample was heated to the IsoLiq. phase and then cooled monotonically, the SmC^* -IsoX phase transition occurred around 386.1 K, as shown in Figure 9(a). On the other hand, Figures 9(b) and 9(c) show results when the sample is heated to the IsoLiq. phase and then cooled but kept in the IsoLiq.- SmC^* phase temperature region for several days before cooling down to the IsoX phase. In this case the SmC^* -IsoX transition occurred at somewhat higher temperature, 387–388 K. Further, the location of the SmC^* -IsoX transition was changed by another unknown factor, probably just an accidental one, as seen as the difference between the results of Figures 9(b) and 9(c), which were resulted from temperature history quite similar to each other. You may recall the fact that the temperature range of SmC^* is dependent on cell thickness, as observed in the dielectric measurements (Figure 2). After all, these results indicate that the SmC^* phase is metastable, and the transition to the IsoX is affected by various extrinsic factors.

3.4 Structure of Bluish-Colored Phase

Although no other DSC peak was observed above the IsoLiq.- SmC^* phase transition, bluish and foggy texture was observed under a microscope near

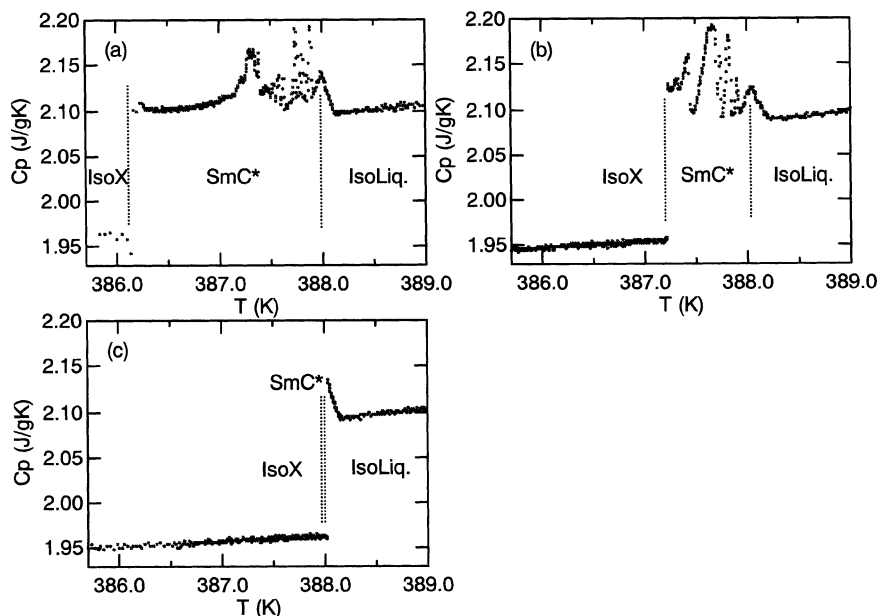


FIGURE 9 Temperature dependence of heat capacity measured after various time intervals.

the transition to SmC^* , suggesting the existence of cholesteric BP phase. In the X-ray diffraction, a clear but broad ring pattern appears at 130°C , as shown in Figure 8(b). This diffraction indicates the existence of a kind of layer structure. The intensity of this ring diffraction gradually decreases with the increase of temperature. According to the analysis of the X-ray diffraction profile, the correlation length was found to reach at least $0.5\ \mu\text{m}$ in the vicinity of the phase transition to SmC^* . This value is quite large compared with that reported by Pansu *et al.* (at most $0.1\ \mu\text{m}$)[4]. Thus, the existence of BP_{sm} is strongly suggested.

The transition from Iso to BP_{sm} was also thermally confirmed by means of AC calorimeter, i.e., a very small and broad peak was observed in a wide temperature range more than 20°C . Details of this thermal analysis was reported in a separate paper[19]. This kind of thermal behavior showing a broad peak is similar to those in the chiral compound showing the BP_{sm} and TGB phases, as reported by Pansu *et al.*[20].

Circular dichroism (CD) measurements were also carried out, as reported in our pervious paper[11]. CD peaks were observed near $300\ \text{nm}$, and the highest intensity was observed just above the phase transition from BP_{sm} to SmC^* . This fact suggests that the structure in this temperature

range already has some helix-related structures before making a transition to SmC* or IsoX. Thus, this blue-colored phase is similar to the blue phase appearing between IsoLiq. and cholesteric phases but is different in the sense that it appears between IsoLiq. and SmC* and thus possesses a layer correlation.

4. CONCLUSION

The structure and dynamics in the optically isotropic liquid crystalline phase (IsoX) exhibited in the novel dichiral compounds with fluorines, (*R*, *S*)-FPPY, were investigated using X-ray, ^{19}F -NMR and dielectric measurements. The dielectric measurement and T_1 and MAS F-NMR measurements in (*R*, *S*)-FPPY certify that the dynamic molecular motion in IsoX is very similar to that in the isotropic liquid. Moreover, results in the X-ray microbeam diffraction together with the existence of circular dichroism clearly indicate a kind of chiral cubic phase belonging to I432. Moreover, the blue colored and foggy texture was observed in the lower temperature range of isotropic liquid. This phase has long range density correlation compared with the normal BP_{sm} and TGB phases, and exhibits a large CD signal due to the macroscopic helical structure, suggesting a new phase. It is also worthwhile to note that this is the first material that stably shows both chiral cubic phases, BP_{sm} and Cub (I432).

REFERENCES

- [1] Goodby, J. W., Waugh, M. A., Stein, S. M., Chin, E., Pindak, R., & Patel, J. S. (1989). *Nature*, **337**, 449.
- [2] Crooker, P. P. (1989). *Liq. Cryst.*, **5**, 751.
- [3] Li, M.-H., Laux, V., Nguyen, H.-T., Sigaud, G., Barois, P., & Isaert, N. (1997). *Liq. Cryst.*, **23**, 389.
- [4] Pansu, B., Li, M. H., & Nguyen, H. T. (1997). *J. Phys. II France*, **7**, 751.
- [5] Pansu, B. & Brelet, E. (2000). *Phys. Rev. E*, **62**, 658.
- [6] Diele, S. & Göring, P. *Handbook of Liquid Crystals*, Vol. 2B, Chapter XIII (Weinheim, Wiley-VCH, 1998).
- [7] Vill, V., Bachmann, F., & Thiem, J. (1992). *Mol. Cryst. Liq. Cryst.*, **213**, 57.
- [8] Yoshizawa, A., Umezawa, J., Ise, N., Sato, R., Soeda, Y., Kusumoto, T., Sato, K., Hiyama, T., Takanishi, Y., & Takezoe, H. (1998). *Jpn. J. Appl. Phys.*, **37**, L942.
- [9] Kusumoto, T., Sato, K., Katoh, M., Matsutani, H., Yoshizawa, A., Ise, N., Umezawa, J., Takanishi, Y., Takezoe, H., & Hiyama, T. (1999). *Mol. Cryst. Liq. Cryst.*, **330**, 221.
- [10] Takanishi, Y., Takezoe, H., Yoshizawa, A., Kusumoto, T., & Hiyama, T., (2000). *Mol. Cryst. Liq. Cryst.*, **347**, 257.
- [11] Takanishi, Y., Ogasawara, T., Yoshizawa, A., Umezawa, J., Kusumoto, T., Hiyama, T., Ishikawa, K., & Takezoe, H., (2002). *J. Mater. Chem.*, **12**, 1325.
- [12] Tokumaru, K., Jin, B., Yoshida, S., Takanishi, Y., Ishikawa, K., Takezoe, H., Fukuda, A., Nakai, T., Miyajima, S. (1999). *Jpn. J. Appl. Phys.*, **38**, 147.

- [13] Yoshida, S., Jin, B., Takanishi, Y., Tokumaru, K., Ishikawa, K., Takezoe, H., Fukuda, A., Kusumoto, T., Nakai, T., & Miyajima, S. (1999). *J. Phys. Soc. Jpn.*, **68**, 9.
- [14] Iida, A., Noma, T., & Hirano, K. (1994). *Ferroelectrics*, **149**, 117.
- [15] Takanishi, Y., Iida, A., Ishikawa, K., Takezoe, H., & Fukuda, A. (1996). *Jpn. J. Appl. Phys.*, **35**, 683.
- [16] Ema, K. & Yao, H. (1997). *Thermochim. Acta*, 3041305 157.
- [17] Diele, S., Brand, P., & Sackmann, H. (1997). *Mol. Cryst. Liq. Cryst.*, **17**, 163.
- [18] Levelut, A. M. & Clerc, M. (1998). *Liq. Cryst.*, **24**, 105.
- [19] Ema, K., Yao, H., Takanishi, Y., Takezoe, H., Kusumoto, T., Hiyama, T., & Yoshizawa, A., (2002). *Liq. Cryst.*, **29**, 221.
- [20] Pansu, B., Li, M. H., & Nguyen, H. T. (1997). *J. Phys. II France*, **7**, 751.